THE ASTRONOMICAL JOURNAL, 120:298–313, 2000 July

2MASS EXTENDED SOURCES IN THE ZONE OF AVOIDANCE

T.-H. JARRETT, T. CHESTER, AND R. CUTRI
Infrared Processing & Analysis Center, MS 100-22, California Institute of Technology, Jet Propulsion Laboratory, Pasadena, CA 91125; jarrett@ipac.caltech.edu, tchester@ipac.caltech.edu, roc@ipac.caltech.edu

S. SCHNEIDER AND J. ROSENBERG
Astronomy Program, University of Massachusetts, Amherst, MA 01003; jessica@phast.umass.edu, schneider@phast.umass.edu

AND

J. P. HUCHRA AND J. MADER
Harvard Smithsonian, CfA, Cambridge, MA 02138; huchra@cfa.harvard.edu, jmader@cfa.harvard.edu
Received 2000 February 16; accepted 2000 March 30

ABSTRACT

A new high-resolution near-infrared mapping effort, the Two Micron All Sky Survey (2MASS), is now underway and will provide a complete census of galaxies as faint as 13.5 mag (3 mJy) at 2.2 μm for most of the sky, and $\sim$12.1 mag (10 mJy) for regions veiled by the Milky Way. This census has already discovered nearby galaxies previously hidden behind our Galaxy and will allow delineation of large-scale structures in the distribution of galaxies across the whole sky. Here we report the detection and discovery of new extended sources from this survey for fields incorporating the Galactic plane at longitudes between 40° and 70°. Follow-up H I 21 cm and optical spectroscopy observations provide positive confirmation for 14 of the new 2MASS galaxies. We perform an internal completeness and reliability analysis for the sample, consisting of 7000 sources in $\sim$1000 deg^2 of area, including galaxies and Galactic nebulae from the W51 giant molecular cloud. The area-normalized detection rate is about one to two galaxies per deg^2 brighter than 12.1 mag (10 mJy), roughly constant with Galactic latitude throughout the "Zone of Avoidance," of which 85%–95% are newly discovered sources. In conjunction with the deep H I surveys, 2MASS will greatly increase the current census of galaxies hidden behind the Milky Way. Moreover, owing to its sensitivity to elliptical and other gas-poor galaxies, 2MASS will provide a key complementary data set to that of the gas-rich–sensitive H I surveys of the Milky Way galaxy, potentially uncovering nearby galaxies critical to the local gravity and mass density fields.

Key words: galaxies: general — H II regions — infrared radiation — ISM: individual (W51) — surveys

1. INTRODUCTION

Over the last two decades astronomers have learned that the local universe exhibits a complex topology, characterized by groups and clusters of galaxies aligned along sheets and filamentary structures. The structures are often portrayed as "walls" of galaxies or "bubbles and voids," with sizes ranging from 30 to 150 $\times$ 10^6 lt-yr across (de Lapparent, Geller, & Huchra 1986; Giovanelli & Haynes 1988; Geller & Huchra 1989; da Costa et al. 1994; Di Nella et al. 1997). Moreover, nearby galaxies, including the Milky Way and Andromeda (M31), exhibit a peculiar flowing motion with respect to the cosmic background radiation, with the signature being a large angular scale dipole feature in the cosmic microwave background (e.g., Smoot, Gorenstein, & Muller 1977). In the simplest of interpretations, the dipole is dominated (after correcting for the motion of the Sun through the Galaxy) by a streaming motion of galaxies toward what is frequently called the "Great Attractor" (Lynden-Bell et al. 1988; Kolatt, Deker, & Lahav 1995), located somewhere behind the Galactic center region, probably associated with the massive rich cluster Abell 3627 at $\sim$5000 km s^{-1}, at $l \sim 325°$, $b \sim -7$ (Kraan-Kortweg et al. 1996).

The velocity field is complicated by infall motion of the Local Group of galaxies toward the nearby Virgo Cluster (Aaronson et al. 1982) as well as a peculiar motion toward the Galactic anticenter region, the so-called local velocity anomaly (Faber & Burstein 1988; Lu & Freudling 1995) and the Puppis constellation, also located deep in the plane of the Milky Way, at $l \sim 240°$, $|b| < 10$ (Lahav et al. 1993; Kraan-Kortweg & Huchtmeier 1992). If galaxies are the tracers of mass in the local universe, then in order to decode these complex phenomena, it is essential that we derive a complete census of galaxies local to the Milky Way.

This objective has been frustrated by the presence of the Galaxy itself—the Milky Way's gas, dust, and stars obscure to one degree or another about one-half of the entire sky, including $\sim$20% that is significantly veiled from view. Traditional visual spectroscopic and imaging surveys have usually avoided the plane of the Galaxy; hence, the "zone of avoidance" (hereafter, ZoA) refers to the region of the sky from 10° to 30° from the Galactic plane at $|b| = 0°$ (the zone also depends on Galactic longitude, with the zone area increasing toward the Galactic center at $l \sim 0°$). As such, not only is a significant fraction of the local universe gravity field undefined, but the observed fraction is split into two disconnected parts, which may lead to biases in interpreting the structure. Once it was realized that galaxies in the ZoA play an important role in deciphering the supergalactic plane and the local universe in general, new methods were utilized to see through the veil of the Milky Way.

Although there are ongoing efforts to penetrate the ZoA down to $|b| \sim 10°$ using deep optical imaging that targets low-obscuration "windows" (e.g., Kraan-Korteweg & Woudt 1999; Kraan-Korteweg et al. 1996), the best solution is to observe the ZoA at longer wavelengths that are less effected by dust attenuation. The *Infrared Astronomical*

Satellite (*IRAS*) provided one of the first uniform and complete, to ~1–2 Jy at 60 mm, windows into the ZoA, revealing many nearby infrared-bright galaxies near or within the Milky Way (Rowan-Robinson et al. 1990; Saunders et al. 1991; Kaiser et al. 1991; Fisher et al. 1995; Lu et al. 1990; Oliver et al. 1996; Canavezes et al. 1998; Branchini et al. 1999). However, far-infrared surveys, such as the *IRAS* 1.2 Jy PSC and the PSCz, are ultimately limited by their poor spatial resolution and bias toward dusty luminous galaxies, such as late-type spirals and starbursts.

One promising approach to finding galaxies in the ZoA is to look for redshifted 21 cm neutral hydrogen line emission (H I). Many studies to detect galaxies in the ZoA in H I have been carried out (Henning 1992; Pantoja et al. 1997; Kraan-Korteweg & Huchtmeier 1992; Lu & Freudling 1995), with some extensive surveys of the ZoA underway, including the Dwingeloo Obscured Galaxy Survey (e.g., Kraan-Korteweg et al. 1994; Henning et al. 1998) and the Parkes multibeam survey (HIPASS; Staveley-Smith 1997; Henning et al. 1999; Juraszek 1999). The H I surveys have been successful at finding new galaxies in the ZoA, including a handful of very large nearby galaxies, such as Dwingeloo 1, located just beyond the Local Group (Kraan-Korteweg et al. 1994). These surveys, however, are sensitive only to gas-rich nearby spirals (e.g., Dwingeloo 1 and Maffei 2), where their sensitivity drops as the inverse square of the distance of the sources. For example, the noise limits of the all-sky Parkes (shallow) survey (Kilborn, Webster, & Staveley-Smith 1999) permit only the detection of a typical spiral with 10^9 solar masses of H I to a redshift of about 2000 km s^{-1}. Deeper surveys in the Galactic plane are now in progress that will achieve better sensitivity, extending the search volume out to 10,000 km s^{-1} for galaxies with very high H I masses (Kraan-Korteweg et al. 1998; Staveley-Smith et al. 1998; Kraan-Korteweg & Woudt 1999).

Near-infrared surveys have the advantage of being sensitive to most types of galaxies, including gas-poor spheroidals. In addition, being imaging surveys, they detect typical spiral galaxies out to ~20,000 km s^{-1} and the largest galaxies about 5 times farther. Tracing elliptical galaxies is important for solving the large-scale gravity and velocity fields in the local universe because they trace the densest regions. The *IRAS* and H I surveys, by contrast, are insensitive to these largest cluster galaxies. Two large near-infrared surveys are currently underway: the Deep NIR Southern Sky Survey (DENIS; Epchtein et al. 1997; Kraan-Korteweg et al. 1998; Staveley-Smith et al. 1998; Kraan-Korteweg & Woudt 1999), and the Two Micron All Sky Survey (hereafter 2MASS; Skrutskie et al. 1997). Both projects nicely complement the *IRAS* and H I surveys, since they are sensitive to both spiral and elliptical-type galaxies as faint as $K = 12$th mag (10 mJy) in the ZoA.

2MASS is a ground-based, imaging survey that utilizes the near-infrared atmospheric band windows at J (1.25 μm), H (1.65 μm), and K_s (2.17 μm). One of the key scientific objectives of 2MASS is to study large-scale structures in the local universe. Near-infrared surveys are able to address these issues owing to their unique properties: (1) e.g., 2MASS is a highly uniform all-sky survey, so a complete census is possible; (2) the mass distribution of galaxies is dominated by the older stellar population, which in turn emit most of their light in the near-infrared; (3) interstellar extinction *within* galaxies is considerably less than that observed at optical wavelengths; similarly, extinction from gas and dust in the Milky Way is greatly reduced in the near-infrared, providing a window into and through the ZoA; (4) the spatial resolution of 2MASS/DENIS allows detection and identification of the more numerous small galaxy members of clusters; and (5) for highly inclined spirals, distances may be inferred using the infrared Tully-Fisher relation.

The combined sensitivity and spatial resolution of 2MASS will lead to detection of over 10^6 galaxies out to redshifts greater than 30,000 km s^{-1} for most of the sky (Jarrett et al. 2000a). In the ZoA 2MASS will discover many new galaxies, including those belonging or in close proximity to the Local Group. For example, a large (~6′ diameter) nearby (775 km s^{-1}) galaxy was recently discovered with 2MASS (Hurt et al. 2000). This paper shows that for the Galactic plane, deep in the ZoA, the combined effects of source confusion and extinction ultimately limit detection to bright, 12–13th mag (5–10 mJy at K band), nearby galaxies, $z \sim 10{,}000$ km s^{-1}, with "normal" early-type morphology, including spirals and ellipticals. The data set and targeted fields are introduced in § 2. In § 3 we present a detailed study of a large piece of sky bounding the ZoA between 40° and 70° Galactic longitude, including extended source counts, completeness and reliability, and color distribution. We illustrate the kinds of extended sources that 2MASS detects in the ZoA, including follow-up H I observations to verify the extragalactic nature of a number of sources. In § 4 we discuss the impact that 2MASS will have upon understanding large-scale structure across the plane of the Milky Way.

2. DATA AND THE FIELD OF STUDY

The 2MASS Second Incremental Data Release includes large portions of the Milky Way, including the region at $40° < l < 70°$ and $|b| < 40°$, that is the targeted area of study presented in this paper. For this longitude range, the ZoA is roughly defined to be the area within 20° of the plane, or comprising about 50% of the field area. The field location with respect to the backdrop of the Milky Way is illustrated in Figure 1. The area is bisected by the Sagittarius tangent arm extending from the Galactic center and incorporates portions of the Cygus, Lyra, Vulpecula, Sagitta, Hercules, Aquila, Delphinus, and Pegasus constellations. The star formation region, W51 molecular cloud complex, lies at the center of the field, $l \sim 49°$, $b \sim -0.^\circ5$. The field was chosen for study owing to its large dynamic range in stellar number density, from a few hundred to tens of thousands of stars per square degree; moreover, it is infused with a diverse population of Galactic sources associated with star formation. It is confusion from foreground stars that ultimately limits the sensitivity and reliability of the extended sources, both Galactic and extragalactic, that can be extracted by 2MASS. Hence, the field of study (Fig. 1) provides a broad test of the ability of 2MASS to detect extended sources subject to vastly different environments and confusion levels. To date, the 2MASS survey has scanned over 1000 deg^2 of the defined area, corresponding to about one-quarter of the total possible area, consisting of ~1880 individual scans (each scan is 6° × 0.°15) determined to be of high quality as measured with photometric and sensitivity proxies.

The region of study ranges in stellar number density (hereafter shortened to "density") from a mere 1000 stars deg^{-2} brighter than 14.0th mag at K_s (1.8 mJy) to an enor-

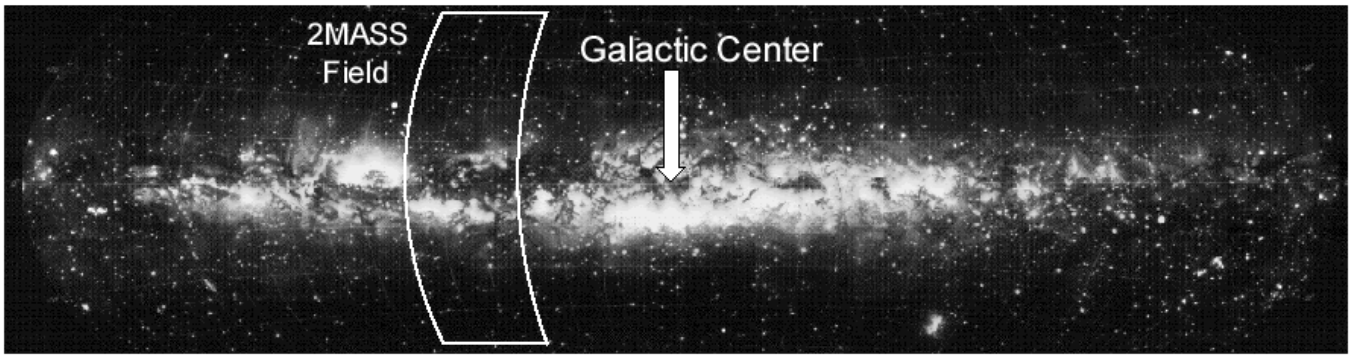

FIG. 1.—Visible Milky Way galaxy. Home to some 400,000 × 10^6 stars, including the Sun, interstellar gas, and dust, nearly all of which are confined to the "disk" or plane of the Galaxy. The Galactic plane, depicted here in a scientifically accurate drawing from the Lund Observatory (by K. Lundmark in 1940) as seen at visible wavelengths, is characterized by patchy and thick dust lanes crossing a very high surface density "disk" of stars. This region fills nearly one-quarter of the observable sky, in effect a giant curtain or veil to the universe beyond the Milky Way. 2MASS will survey the entire sky, revealing both deeply embedded star formation regions and galaxies located beyond the Milky Way. The region of the plane relevant to this work is indicated with a box, located between 40° and 70° in longitude from the Galactic center, in the Sagittarius Arm Tangent.

mous 40,000 stars deg^{-2} near the Galactic plane. Stars typically outnumber galaxies by a factor of 100–10,000 in the ZoA; consequently, it is a challenge to find galaxies in these crowded fields. The 2MASS project employs automated star-galaxy discriminator techniques to reduce the ratio of stars to galaxies to a more manageable 2:1 or 1:1 ratio (detailed in Jarrett et al. 2000a). It is then a straightforward process to cull out the remaining nonextended sources (such as triple stars) using visual examination of images, or more sophisticated automated methods, such as decision trees or neural nets. We also compared our source lists with astronomical databases to identify previously cataloged objects, such as planetary nebulae.

2MASS supplies a variety of integrated flux measurements for a given extended source. In this study we use the integrated flux based on the elliptical aperture best fit to the

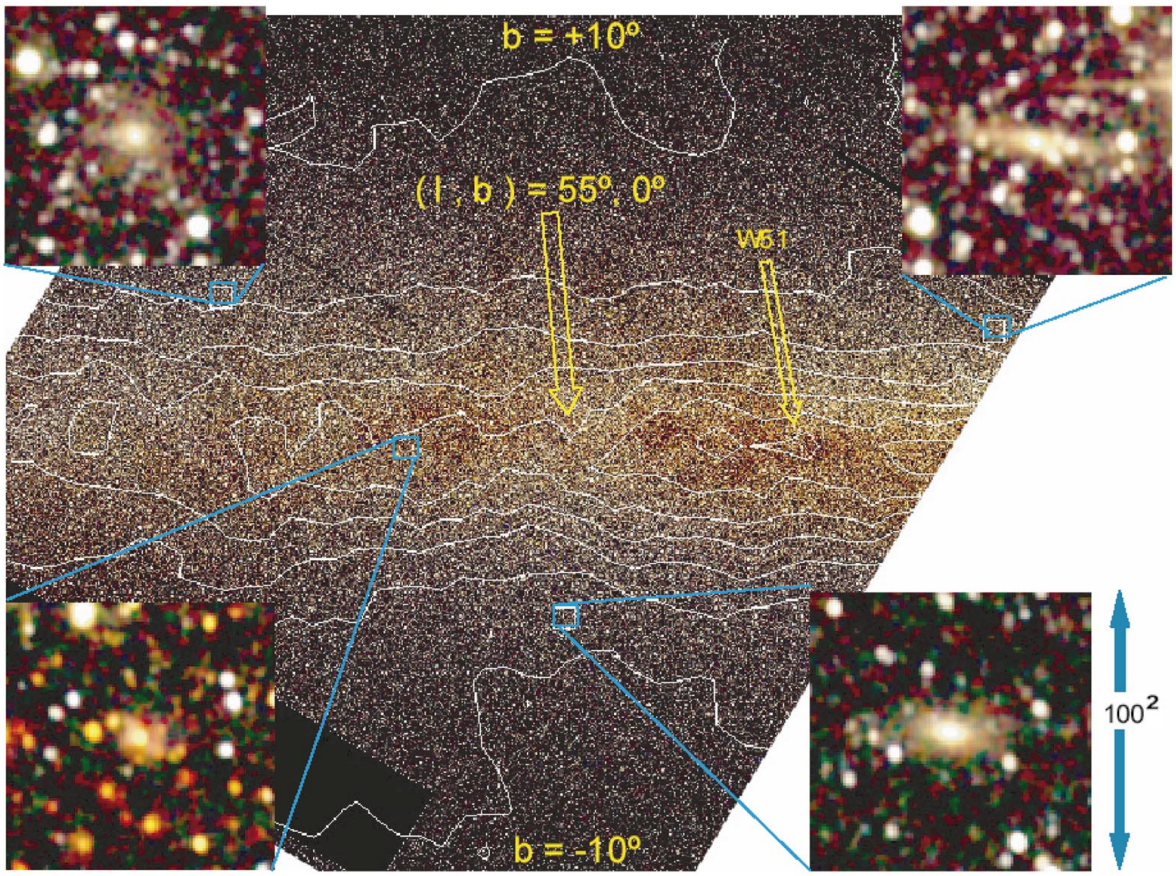

FIG. 2.—2MASS view of the Milky Way near $l \sim 55°$, spanning some 500 deg^2. The RGB color composite images are derived from assigning the color blue to the J band (1.2 μm), green to the H band (1.6 μm), and red to the K_s band (2.2 μm). Note the effects of dust-extinction reddening near $b = 0°$ and in the direction of the Galactic center (to the west, or right-hand side of figure). The extinction roughly tracks to the atomic hydrogen column density, represented by the white contours (derived from the maps of Hartmann & Burton 1997), which are in the range 1.8–14 × 10^{21} cm^{-2} (in steps of 2.1 × 10^{21} cm^{-2}). Inset images represent a galaxy (*lower right*) and a probable H II region (*lower left*) that illustrate the ability of 2MASS to peer into and through the Milky Way. Missing or low-quality image data appear as black strips.

K_s-band isophote corresponding to 20.0 mag arcsec^{-2} in surface brightness (roughly equivalent to 1 σ of the rms background noise in the K_s-band image). The same "fiducial" aperture (position, size, and orientation) is applied to each band, allowing cross-comparison between bands.

A three-color JHK_s mosaic of the subsection field concentrating on the most extreme ZoA, $|b| < 10°$, is shown in Figure 2. The stellar foreground confusion is noticeably most severe near $b = 0°$. Nonetheless, 2MASS is able to find extended sources peering through the Milky Way: four typical galaxy detections are highlighted in Figure 2. The presence of gas and dust is clearly seen near the Galactic plane, $|b| < 5°$, with an H I gas column density gradient vectored west toward the Galactic center.

The major limitation to galaxy detection by 2MASS in the ZoA is "confusion" noise from stars. The confusion noise becomes appreciable within an area $\pm 5°$ of the Galactic plane (Fig. 2). The end result is a loss of sensitivity as the surface density of stars increases exponentially. Correspondingly, a profusion of multiple star groupings, including double and triple stars, mimic galaxies and are falsely identified by the automated extended source detection and extraction routines. Nevertheless, 2MASS can identify galaxies as faint as 13th mag at K_s ($\sim$4.4 mJy) for $|b| > 5°$–$10°$, and as faint as 12.1 mag at K_s ($\sim$10 mJy) down to $|b| \sim 2°$–$3°$. A different sort of problem arises from the fact that galaxies and Galactic extended sources are sometimes difficult to discriminate from each other based on their morphology and colors. H II regions are found predominantly at Galactic latitudes less than 3°. For this study, the number of extended sources brighter than $K_s = 13$th mag ($\sim$4.4 mJy), including galaxies, Galactic nebulae, and multiple groupings of stars, is $\sim$7000 in total.

Finally, to establish firmly the extragalactic nature of 2MASS extended sources deep in the ZoA, we are carrying out systematic follow-up observations of sources brighter than $\sim$12.5 at K_s using radio telescopes at Arecibo and Nançay, and optical telescopes at the F. L. Whipple (FLWO) and Palomar observatories. Here we report preliminary (0.38–0.75 μm) spectroscopic results for eight sources using the FLWO Tillinghast reflector, where measured redshift uncertainties range between 20 and 40 km s^{-1}, and for an additional eight sources (mostly invisible at optical wavelengths due to dust obscuration) 21 cm spectroscopy using the new Gregorian reflector system on the 305 m Arecibo telescope, achieving 21 km s^{-1} resolution after smoothing with 0.9 mJy rms.

3. RESULTS

3.1. *Source Classification*

Our objective is to assess the quality of the 2MASS extended-source data, to forecast the quality of the catalogs that are ultimately to be produced, and to identify galaxies located behind the Milky Way. To this end, we have collected all of the sources in the defined area (§ 2) that are deemed "extended" (i.e., resolved) with respect to the point-spread function (PSF) by the 2MASS project, as of the Second Incremental Data Release.[1] We have looked at all sources brighter than 13th mag at K_s, which is slightly fainter than the 2MASS confusion noise limit in the ZoA.

To determine the nature of the object, in particular, extragalactic versus stellar, we have visually examined each source using 2MASS data. We compare the NIR images with independently acquired optical-wavelength image data. The Digitized Sky Survey (DSS), for example, is well matched in surface brightness and resolution to that of 2MASS for normal-colored galaxies. Some sources can be cross-identified with astronomical databases (e.g., NED, ZCAT, and SIMBAD). Finally, for some cases in which the reddening is severe (e.g., at $|b| < 5°$–$10°$, the DSS is largely ineffective), we obtained additional radio, optical, or deep infrared data. Previously identified/cataloged sources in the ZoA tend to be Galactic nebulae, such as H II regions, which have very red colors, $J - K_s > 1.5$, redder than most 2MASS extragalactic sources. It is not possible to clearly identify every source detected in the survey. In particular, "fuzzy" objects at very low Galactic latitude are *likely* to be Galactic nebulae (e.g., H II regions), representing the primary "contaminant" to any *extragalactic* catalog that extends below $|b| < 3°$.

For simplicity and owing to the difficulty with discriminating galaxies from Galactic nebulae, we visually categorize extended source candidates as either (1) extended (including galaxies and Galactic nebulae), (2) false (double and triple stars, artifacts), and (3) unknown. Identification of multiple stars is generally straightforward owing to their high surface brightness and relatively "blue" $J - K_s$ colors with respect to extragalactic objects, which suffer a greater level of reddening due to foreground Galactic extinction. Artifacts arise from two primary sources: bright stars (e.g., Altair and Vega are in close proximity to the field of study) and transient events (e.g., meteor streaks); see Jarrett et al. (2000a) and the 2MASS Explanatory Supplement[2] (Cutri et al. 2000) for more details. Most of the artifacts can be eliminated by applying optimized algorithms that recognize their signatures, but there will always be artifacts that are difficult to eliminate with automated routines. Although time-consuming, visual inspection remains the most reliable method for artifact elimination.

With this classification scheme we are able to assess the absolute reliability and internal completeness of a 2MASS extended source "catalog," as well as to quantify the color gradient of galaxies with Galactic latitude. One should bear in mind that the final 2MASS extended source catalog will contain mostly (>98%) galaxies at $|b| > 20°$, a mixture of ($\sim$90%) galaxies and nonextended sources ($\sim$10%) at $5° < |b| < 20°$, and finally, both extragalactic ($\sim$40%) and Galactic extended sources ($\sim$40%) and artifacts ($\sim$10%–20%) at $|b| < 5°$, for a large range in longitude. There are inevitably small patches of the Galactic plane where the reliability is likely to be very poor; for example, in the Galactic center region, $350° < l < 10°$, the confusion noise overwhelms any attempt at distinguishing extended sources from foreground stars.

3.2. *A Montage of Galaxies and Nebulae in the ZoA*

A colorful "zoo" of galaxies is identified in our ZoA field, exhibiting a wide mix in morphology and surface bright-

[1] Available at http://www.ipac.caltech.edu/2mass/releases/second/index.html.

[2] On line at http://www.ipac.caltech.edu/2mass/releases/docs.html.

ness. Deep in the Galactic plane we encounter extremely red and bright fuzzy objects, many of which are associated with the W51 molecular cloud complex. Examples of typical extended sources found in this ZoA region are shown in Figure 3, with their basic infrared parameters given in Table 1. This sample represents only 1% of the total number of galaxies and nebulae brighter than 12th mag (10 mJy) at 2.2 mm identified in the field between 40° and 70° longitude. At the "gray" edge of the ZoA (e.g., Fig. 3, *upper*), about one-quarter 2MASS extended sources are previously cataloged galaxies (see § 3.3.4 for details). As the source density and visual extinction increase (see Fig. 3, *bottom*), only a few cataloged objects remain—mostly faint *IRAS* point sources—precisely where 2MASS will greatly extend our current knowledge of the ZoA.

The 2MASS extended sources have intrinsically red colors, $J-K_s > 1$ (§ 3.3.1; see also Jarrett et al. 2000a), which make them stand out compared to the foreground stellar population. In the ZoA, interstellar reddening amplifies this color contrast, except in the unusual case in which stellar light contamination from the foreground population will slightly offset the measured galaxy colors toward the blue: for example, the galaxy cores of objects 10 and 23 in Figure 3 are contaminated by foreground "blue" stars. The 2MASS processing attempts to remove automatically as much foreground contaminant light as possible by identifying point sources and subtracting their light profiles (Jarrett et al. 2000a). Most of the galaxies in Table 1 have been followed up with deeper imaging and spectroscopic data, detailed below.

The H I observation galaxies were selected based on their morphology: spiral galaxy profiles and surface brightness that would suggest gas-rich content. The resultant heliocentric redshifts and line widths for the sources are given in Table 1. One galaxy candidate did not have an H I detection, which means either the source is (1) a gas-poor early-type spiral or elliptical galaxy, (2) a Galactic extended source containing little neutral atomic hydrogen, or (3) outside the range of redshifts $0 < cz < 10{,}000$ km s^{-1} surveyed. Several large, greater than 90″ in diameter, galaxies are newly discovered, and we have obtained H I line emission profiles (see Table 1). One is a very bright early-type spiral, $K \sim$ 9th mag: object 13 from Figure 3; note that at least 15% of the flux is cut off owing to the western image edge. Likewise, several other new H I–confirmed galaxies are located deep in the ZoA, the largest of which is ~70″ in size based on the 20 K_s mag arcsec^{-2} isophote. We highlight this galaxy in Figure 4.

The galaxy (object 26, Fig. 3) is located at a Galactic latitude of 2°.6. In Figure 4 we compare the 2MASS infrared with the Digitized Sky Survey optical image to demonstrate the effect of extinction on the surface brightness of the background galaxy. It has a K_s brightness of 10.3 mag (54 mJy), and an unusually red $J-K_s$ color of 1.51 mag. The galaxy appears to be an ~Sb or later type spiral, from which we would expect an intrinsic color of between 0.9 and

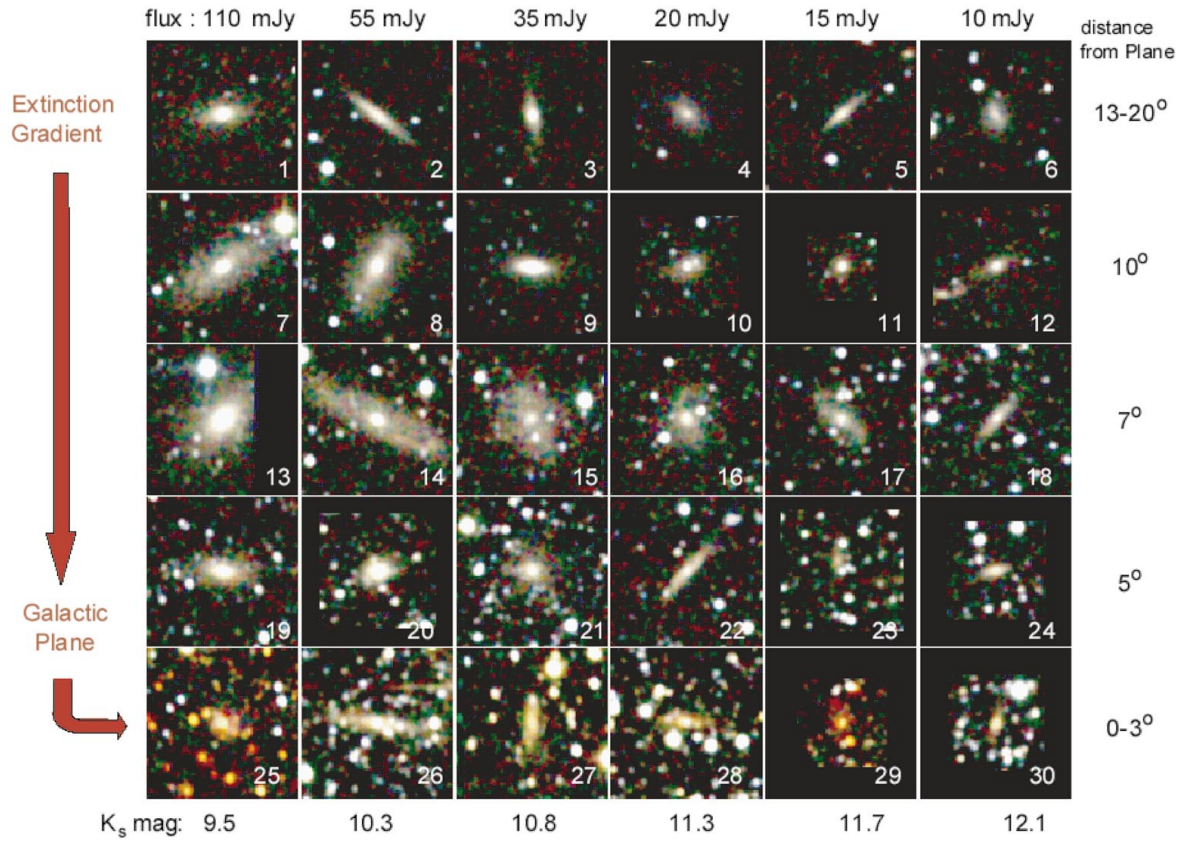

FIG. 3.—Sample of galaxies and extended sources seen through the Milky Way at the 2MASS near-infrared bands. Each image is 90″ in angular size. The RGB color-composite images are ordered in decreasing (*left to right*) total integrated flux ranging from 110 to 10 mJy (corresponding to a K_s magnitude range from 9.5 to 12.1), and in increasing stellar surface density or dust obscuration (*top to bottom*), ranging in $|b|$ from 20 to 0°. See Table 1 for measured parameters.

TABLE 1

PARAMETERS OF 2MASS EXTENDED SOURCES IN THE ZOA

Index	R.A.	Decl.	b	K_s	$J-K_s$	cz	W50	$M_{\rm H\,I}$	Catalog	References
1	306.60947	15.01784	−13.2	10.66	1.09	8506			CGCG	
2	309.92590	13.96138	−16.4	11.30	1.18	6299			CGCG	
3	311.28094	13.39664	−17.8	11.54	1.19	8393			2MASS	
4	311.23340	13.36182	−17.8	11.92	0.96	19321			2MASS	
5	310.60028	13.73427	−17.1	12.06	1.10				2MASS	
6	279.99750	23.87788	13.0	12.19	0.89	4668			CGCG	1
7	281.98737	22.94255	11.0	10.05	0.96	4359			UGC	2
8	282.90720	23.63469	10.5	10.20	1.12	4575	137	2.8	UGC	3
9	282.01831	19.03255	9.3	10.41	1.12	5156			2MASS	
10.....	282.32553	22.42205	10.5	11.72	1.13	?			2MASS	
11.....	300.34976	12.68106	−9.3	12.00	1.28	25405			2MASS	
12.....	282.27026	22.33636	10.5	12.13	1.18				2MASS	
13.....	284.89490	19.10603	6.9	9.24	?	8554	189	8.2	2MASS	
14.....	284.94644	18.83051	6.7	9.84	1.22	4689	548	6.3	IRAS	3
15.....	284.90173	19.42743	7.0	10.32	1.12	3117	264	5.8	UGC	4
16.....	299.93231	14.76543	−7.8	10.91	0.94	4430			CGCG	5
17.....	284.23566	17.96214	6.9	11.32	0.90	4799	283	0.67	2MASS	
18.....	281.45422	14.09969	7.6	11.80	1.16	8519	219	2.2	2MASS	
19.....	297.61945	18.37758	−4.1	10.39	1.38	3975	366	3.9	IRAS	3
20.....	284.82419	13.27716	4.3	10.50	1.37	7309			IRAS	6
21.....	295.04672	29.28221	3.4	10.73	1.13				2MASS	
22.....	285.15134	18.40906	6.3	11.51	1.33	7073	388	3.0	2MASS	
23.....	284.16830	13.20656	4.8	11.88	1.30				2MASS	
24.....	288.23611	22.56506	5.6	12.12	1.42	8979			2MASS	
25.....	295.95224	23.48859	−0.2	10.29	2.65	0			IRAS	7
26.....	286.57559	12.93881	2.6	10.30	1.51	2722	288	1.3	IRAS	
27.....	288.85568	16.92184	2.5	10.91	2.13	6551	487	3.8	IRAS	
28.....	294.38489	23.74393	1.2	11.01	2.12	∼4000			2MASS	
29.....	294.66907	21.82365	0.0	11.40	3.64	0?			IRAS	7
30.....	291.54456	21.98348	2.6	11.99	1.97				2MASS	

NOTES.—Index is identifying number in Fig. 3. R.A. and decl. are the equatorial coordinates in degrees (J2000). b is the Galactic latitude coordinate. 2MASS K_s mag and $J-K_s$ color. cz is the heliocentric redshift in km s^{-1}. W50 is the 50% H I velocity widths in km s^{-1}. Atomic hydrogen mass, $M_{\rm H\,I}$, given in units of $10^9\,M_0$, assuming $H_0 = 75$ km s^{-1} Mpc^{-1}. For source 10, spectroscopic measurements indicate that a foreground star is located directly in front of the galaxy core.

REFERENCES.—(1) Marzke et al. 1996; (2) de Vaucouleurs et al. 1991; (3) Lu et al. 1990; (4) Schneider et al. 1992; (5) Fisher et al. 1995; (6) Nakanishi et al. 1997; (7) probable Galactic reflection nebula.

1.1. The inferred reddening is therefore approximately 0.4–0.6 mag in $J-K_s$, corresponding to a total visual extinction of 3–4 mag—the visual light is attenuated by a factor of 15–40, while the 2.2 μm light is attenuated by only a factor $\sim$2. We may compare this rough empirical estimate with what is deduced from coarse-resolution H I, *IRAS*, and *COBE* surveys of the field, all of which trace the interstellar dust extinction to one degree or another. The H I column density, obtained from the Dwingloo H I survey; Hartmann & Burton (1997), along the line of sight to the galaxy is 0.686×10^{22} cm^{-2}, translating to a visual extinction of $\sim$3.6 mag (assuming $A_v = N_{\rm H\,I} \times 5.3 \times 10^{-22}$ cm^2; see Bohlin, Savage, & Drake 1978). At considerably better spatial resolution, *IRAS* and *COBE*/DIRBE far-infrared maps suggest that the visual extinction is slightly higher, at $\sim$4.9 mag. The far-infrared derived extinction implies that, based on its infrared morphology (see Jarrett 2000), the galaxy is even bluer and of a later type than crudely estimated. Correcting for extinction, the K_s-band isophotal integrated flux of the galaxy becomes 9.6–9.9 mag (75–100 mJy), suggesting that it is located nearby if we assume an L^* luminosity.

The galaxy has a strong H I detection (Fig. 4, *top* and Table 1 for the line flux), indicating that it is indeed a nearby gas-rich spiral at 2722 km s^{-1}. In addition, we have obtained higher spatial resolution K_s-band (2.2 μm) observations with the Palomar 200 inch (5 m) telescope to gauge more accurately the morphology and extent of the galaxy. These data, presented in Figure 5, achieve a sensitivity limit of 21.6 mag arcsec^{-2} (1.6 mJy arcsec^{-2}) in surface brightness, or about 10 times fainter than the 2MASS limit. The deep K-band images corroborate the 2MASS finding of a late-type spiral galaxy with a highly inclined orientation. The light profile exponentially extends down to $\sim$21 mag arcsec^{-2} (2.8 mJy arcsec^{-2}), translating to a total size of $\sim 70''$ as measured at 2.2 μm.

Finally, to illustrate that 2MASS will adeptly detect Galactic nebulae, in addition to extragalactic fuzz, we show the 2MASS three-color wide-field image of the W51 giant molecular cloud complex (Fig. 6). Both in size and mass, W51 is one of the most significant GMCs in the Milky Way and, not surprisingly, is undergoing a vigorous starburst (Carpenter & Saunders 1998; Koo 1997, 1999). The 2MASS automated extended source detector splits the W51 complex into dozens of smaller ($<1'$) sources, including dense star clusters, H II regions, compact radio sources (demarked in Fig. 6), diffuse nebulae, and multiple "minicluster" groupings of stars. For the region studied in this paper, the W51 complex dominates the extended source number counts for $|b| < 2^\circ$ (see § 3.3.3 below).

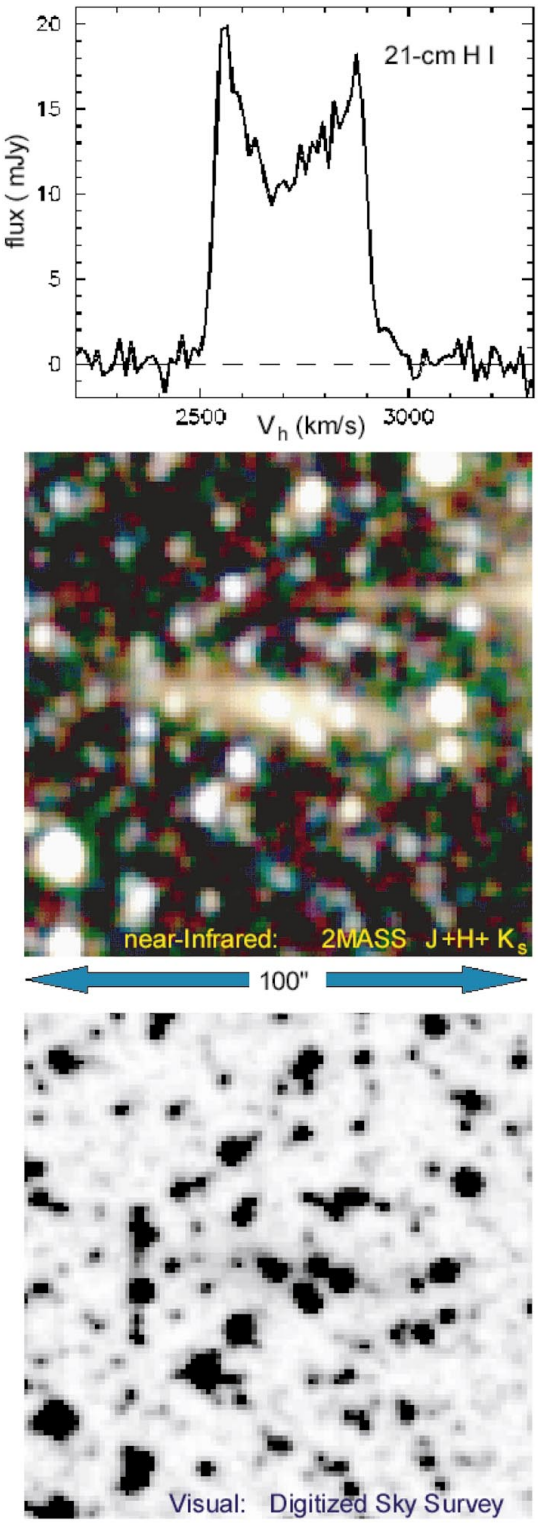

FIG. 4.—Newly confirmed galaxy deep in the Galactic plane, 46° longitude, +2°.6 latitude (2MASS XI1906181+125619 = IRAS 19039+1251; see Table 1). 21 cm H I observations verify the extragalactic nature of the object (*top*), showing the classic double-peak profile of a spiral. At near-infrared wavelengths (*middle*), the galaxy appears to be a Sb or later type spiral highly inclined to our line of sight. For comparison, the bottom panel shows the same region as seen at visual wavelengths, from the Digitized Sky Survey, showing the galaxy to be mostly invisible due to the dust obscuration from the foreground Milky Way.

3.3. *Constructing an Extended Source Catalog*

To demonstrate the usefulness of 2MASS in probing through the ZoA, in this paper we construct an extended source "catalog" for sources brighter than 13th mag (4 mJy) located between 40° and 70° Galactic longitude, and ±40° latitude. The catalog can then be evaluated for completeness and reliability, and finally basic global measurements may be carried out.

The 2MASS extended source *database* is designed to err on the side of completeness, particularly for fields subject to high source confusion. Consequently, in order to derive a *reliable catalog* of extended sources in the ZoA, it is necessary to apply thresholds on key star-galaxy discrimination parameters and further to cull out artifacts by masking large areas around bright stars. The most powerful parameter that separates galaxies from stellar sources is the "gscore" (see Jarrett et al. 2000a, 2000b). This parameter is derived from a machine-assisted oblique decision tree network that utilizes a nine-dimensional parameter space, including the radial "width," intensity-weighted moments, area, symmetry, brightness, and $J-H$ and $H-K_s$ colors of the object. As noted earlier, color is an effective separator between foreground stars and background-reddened galaxies. The "gscore" ranges from 1 = extended to 2 = pointlike. A "gscore" threshold of 1.4 turns out to be a good compromise between improved reliability and stable completeness.

After applying this threshold and masking regions around bright stars ($K_s < 5$th mag) appropriate to the confusion noise level, the overall reliability of the *catalog* is typically better than 90% for $|b| > 10°$. Double stars account for most of the nonextended "contamination" to the catalog, while particularly stubborn artifacts account for 1%–3% of the total. For ~1000 deg^2 of area, we catalog ~7000 extended sources with $K_s < 13$ (4 mJy), and ~2000 with $K_s < 12.1$ (10 mJy). A sky plot of the sources is given in Figure 7, where the left-hand panel corresponds to $K_s <$ 12.1 mag and the right-hand panel to $K_s < 13.0$ mag. The gray regions denote areas that either have yet to be surveyed by 2MASS or have been observed but whose data was deemed poor quality (and are scheduled for future reobservation). The diamond symbols represent cataloged galaxy clusters. Note the dense clustering of sources at northern latitudes, from 20° to 40°; in §§ 3.3.3 and 4 we will address this clustering. Near the Galactic plane, the distinct cluster of points near $l \sim 50°$ and $b \sim -1°$ corresponds to W51 (Fig. 6). Note the apparent decreasing completeness starting at $|b| < 10°$ for $K_s < 13$ (Fig. 7, *right*). For $K_s <$ 12.1 (Fig. 7, *left*), however, the catalog is much more uniform throughout, suggesting that 2MASS is complete for these flux levels.

In order to access asymmetries in the number counts above and below the Galactic plane, we split the source catalog into "northern" and "southern" hemisphere components. Table 2 (north) and Table 3 (south) detail the key global properties of the catalog, including the stellar number "density" (stars per deg^2 brighter than 14th mag at K_s), area (deg^2), mean $J-K_s$ color, mean "H I" gas column density ($\times 10^{21}$ atoms cm^{-2}; derived from the maps of Hartmann & Burton 1997), total number of extended source candidates ("Nx"), completeness ("C"), reliability ("R"), and area-normalized source "counts" (cumulative number deg^{-2}). A cautionary note about the area normal-

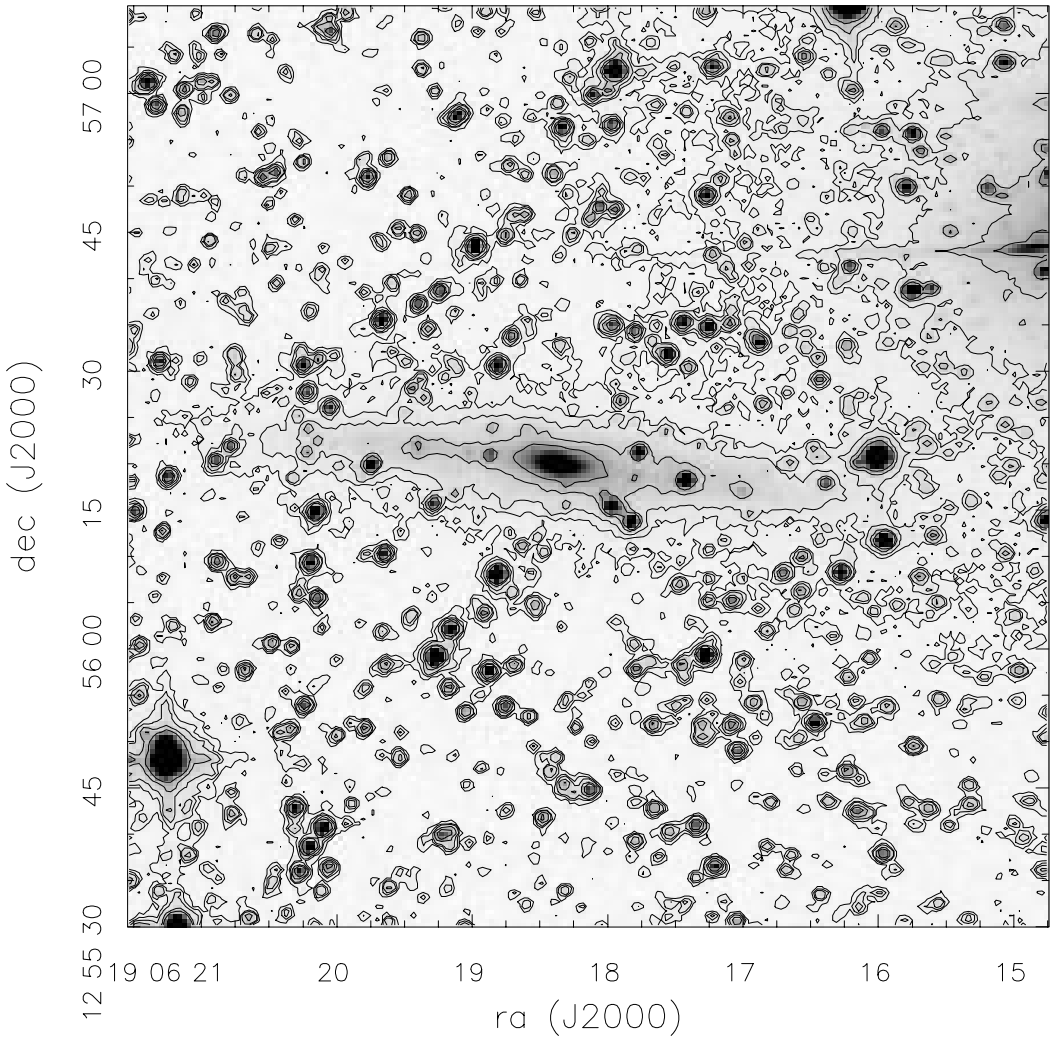

FIG. 5.—Deep K_s band image of 2MASS XI1906181+125619 (see Fig. 4) acquired with the Hale 200 inch (5 m) telescope and the Prime Focus Infrared Camera. The surface brightness sensitivity limit (1 σ) is 21.6 mag arcsec^{-2}, (1.6 μJy arcsec^{-2}), or about 10 times fainter than 2MASS. Surface brightness contours correspond to K_s = 20.8, 19.0, 18.3, 17.3, and 16.5 mag arcsec^{-2}, or a flux range between 3.4 to 180 mJy arcsec^{-2}.

ization: arriving at the correct integrated area for a given latitude interval requires great care, including corrections for coverage gaps, scan-to-scan overlap, masked circular areas due to moderately bright stars (5th < K_s < 9th mag), and masked areas (both circular and rectangular) due to bright stars (K_s < 5th mag). A more detailed prescription for computing the areal coverage for 2MASS extended source data is given in Jarrett et al. (2000b).

TABLE 2

EXTRAGALACTIC AND GALACTIC EXTENDED SOURCE COUNTS: $b > 0°$

					$K_s \leq 13.0$				$K_s \leq 12.1$			
b RANGE	AREA (deg^2)	DENSITY	$J-K_s$	H I	Nx	C	R	Counts $\pm$ Error	Nx	C	R	Counts $\pm$ Error
0.0–2.5	12.2	4.47	1.83	11.3	48	0.90	0.36	3.54 $\pm$ 0.54	47	0.89	0.40	3.44 $\pm$ 0.53
2.5–5.0	24.4	4.19	1.35	4.03	88	0.93	0.61	3.35 0.38	54	0.94	0.70	2.09 $\pm$ 0.29
5.0–7.5	27.9	3.93	1.14	2.54	155	0.95	0.84	5.30 $\pm$ 0.44	36	0.97	0.78	1.26 $\pm$ 0.21
7.5–10.0	30.4	3.71	1.16	1.71	209	0.95	0.95	6.53 $\pm$ 0.47	56	0.91	0.91	1.68 $\pm$ 0.24
10.0–13.0.....	40.9	3.58	1.10	1.13	396	0.95	0.99	9.13 $\pm$ 0.48	80	0.94	0.99	1.83 $\pm$ 0.21
13.0–16.0.....	33.6	3.45	1.09	1.09	331	0.95	0.99	9.37 0.53	79	0.96	1.00	2.26 $\pm$ 0.26
16.0–20.0.....	54.	3.32	1.10	0.83	634	0.99	1.00	11.61 $\pm$ 0.46	170	0.99	0.99	3.11 $\pm$ 0.24
20.0–27.0.....	88.2	3.17	1.08	0.50	835	0.99	1.00	9.40 $\pm$ 0.33	193	0.99	1.00	2.17 $\pm$ 0.16
27.0–35.0.....	117.9	3.00	1.11	0.41	1131	1.00	0.99	9.61 $\pm$ 0.29	335	1.00	0.99	2.84 $\pm$ 0.16
35.0–40.0.....	67.9	2.90	1.05	0.20	874	1.00	1.00	12.87 $\pm$ 0.45	234	0.99	1.00	3.45 $\pm$ 0.23

NOTES.—Density is the number of stars per square degree brighter than 14th mag at K_s. H I is the atomic hydrogen column density ($\times 10^{21}$ atoms cm^{-2}; derived from the maps of Hartmann & Burton 1997). Nx is the total number of extended source candidates. C is the internal completeness and R is the reliability. Counts is the area normalized extended source counts (cumulative number per deg^2).

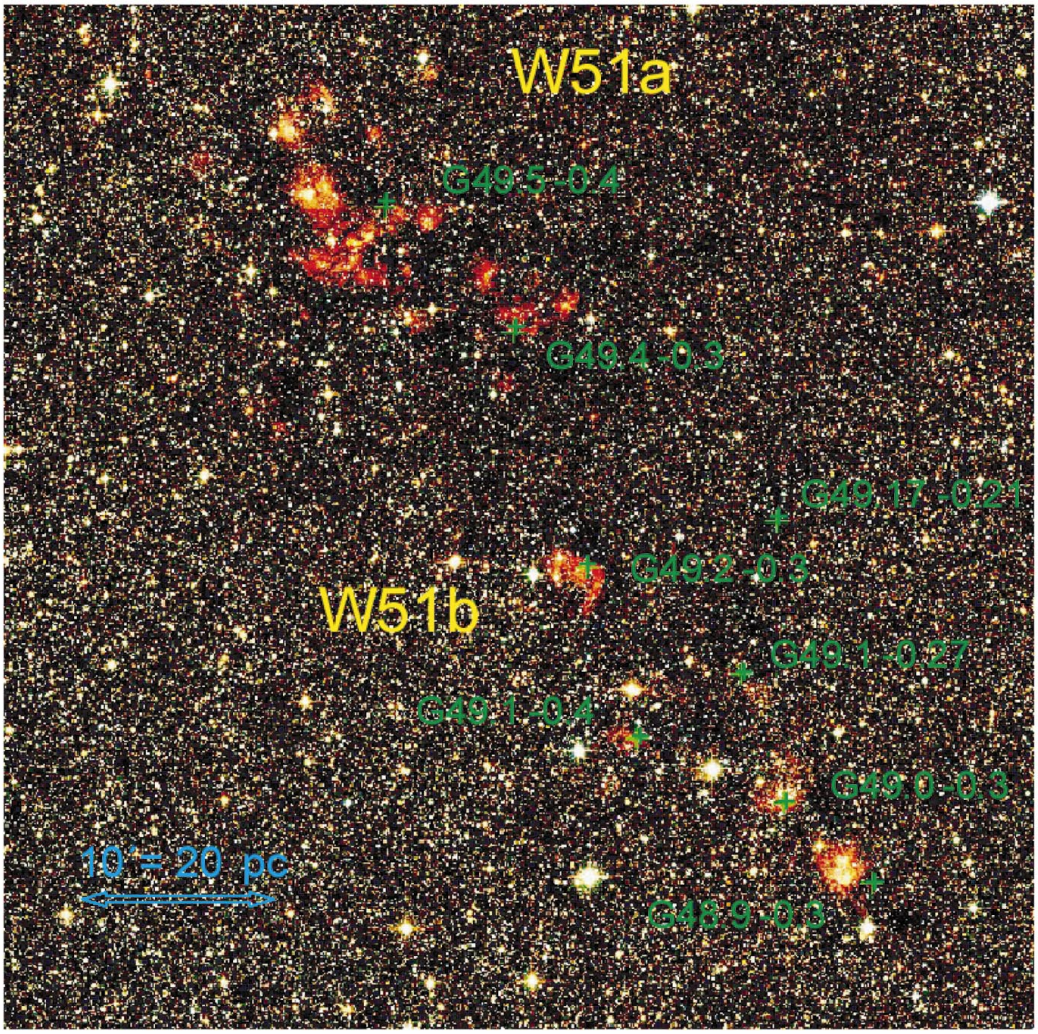

FIG. 6.—W51 molecular cloud complex as seen in the J, H, and K_s color composite. The field angular size is $\sim 45' \times 50'$, shown with an equatorial coordinate projection centered at $18^h23^m13^s.1$, $+14°18'49''$, corresponding to a Galactic coordinate position of ($49°.26$, $-0°.37$). A number of prominent compact radio sources are indicated with green cross symbols (see also Carpenter & Sanders 1998; Koo 1997, 1999). A physical size scale is shown assuming a distance of 7.0 kpc to W51a.

3.3.1. *Extinction and Color versus Galactic Latitude*

The mean $J-K_s$ color for the northern and southern catalog is shown in Figure 8 (*upper panels*), where the filled circles correspond to the north ($b > 0°$) and the open circles to the south ($b < 0°$). Here we have computed the mean color within the specified latitude range (see Table 3) and for $40° < l < 70°$. For comparison, the corresponding mean hydrogen gas column density is also shown (solid line denotes the north, dotted line the south). The atomic gas serves as a proxy measure to the interstellar dust extinction

TABLE 3

EXTRAGALACTIC AND GALACTIC EXTENDED SOURCE COUNTS: $b < 0°$

b RANGE	AREA (deg^2)	DENSITY	$J-K_s$	H I	$K_s \leq 13.0$				$K_s \leq 12.1$			
					Nx	C	R	Counts $\pm$ Error	Nx	C	R	Counts $\pm$ Error
0.0 to -2.5	15.5	4.43	2.56	9.57	70	0.86	0.38	3.88 ± 0.50	63	0.84	0.39	3.41 ± 0.47
-2.5 to -5.0	14.6	4.13	1.32	3.97	51	0.92	0.73	3.21 ± 0.47	19	0.89	0.74	1.17 ± 0.28
-5.0 to -7.5	9.8	3.89	1.19	2.15	63	0.95	0.90	6.12 ± 0.79	11	1.00	0.92	1.12 ± 0.34
-7.5 to -10.0	12.4	3.72	1.13	1.54	99	0.96	0.95	7.67 ± 0.79	17	1.00	0.94	1.37 ± 0.33
-10.0 to -13.0.....	23.6	3.59	1.10	1.02	202	0.96	0.98	8.22 ± 0.59	44	0.98	1.00	1.82 ± 0.28
-13.0 to -16.0.....	20.0	3.46	1.09	0.88	133	0.95	0.97	6.35 ± 0.57	35	0.97	0.92	1.70 ± 0.29
-16.0 to -20.0.....	32.6	3.35	1.05	0.76	237	0.96	1.00	7.01 ± 0.47	61	0.92	1.00	1.72 ± 0.23
-20.0 to -27.0.....	64.7	3.21	1.13	0.62	499	0.99	1.00	7.64 ± 0.36	172	1.00	0.99	2.66 ± 0.20
-27.0 to -35.0.....	71.6	3.07	1.09	0.53	465	1.00	1.00	6.54 ± 0.31	131	1.00	1.00	1.83 ± 0.16
-35.0 to -40.0.....	40.4	2.94	1.09	0.50	255	1.00	1.00	6.32 ± 0.41	53	1.00	1.00	1.31 ± 0.18

NOTES.—See Table 2 notes.

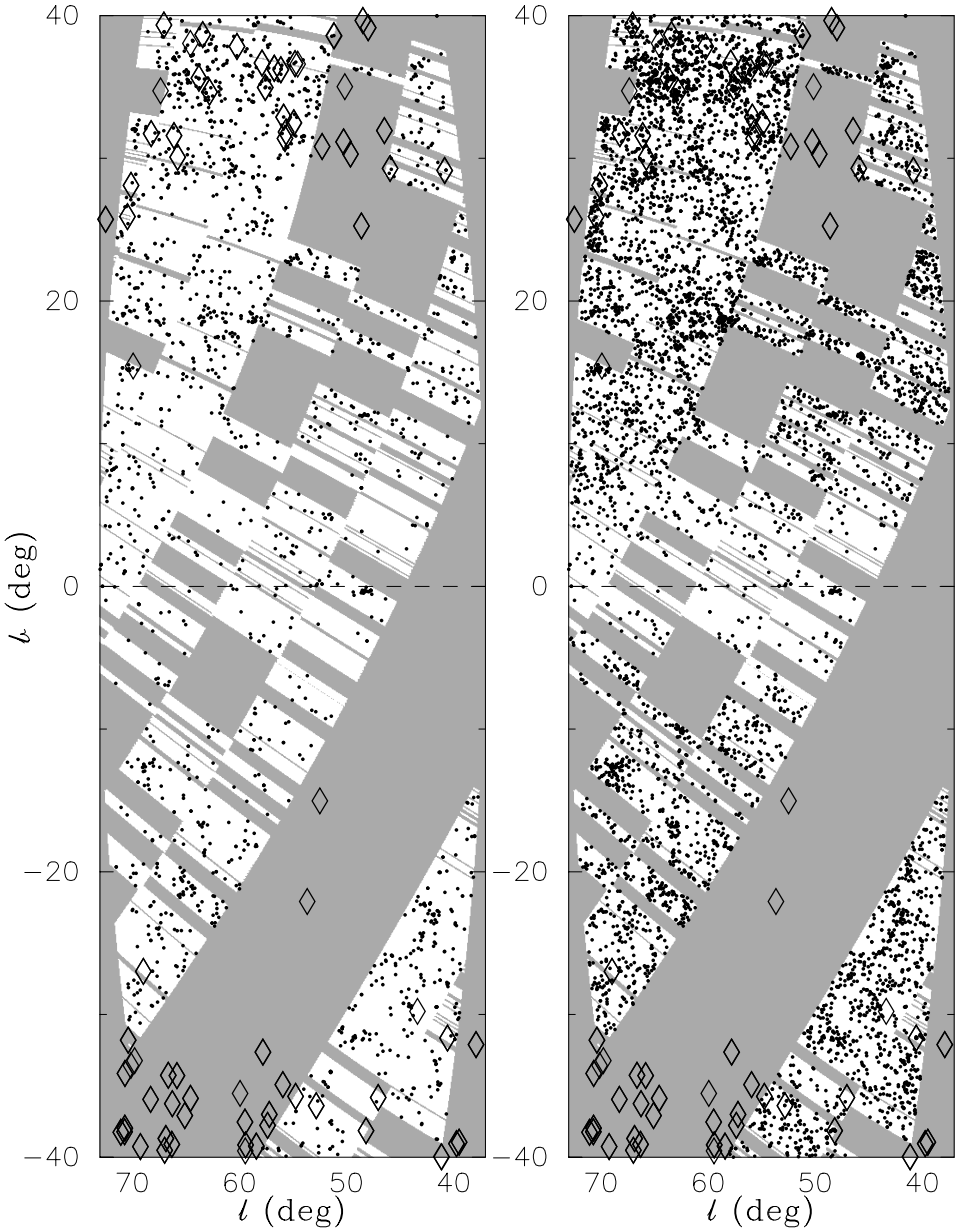

FIG. 7.—Distribution in Galactic coordinates of (*left*) ~1900 galaxies and extended sources in the ZoA brighter than $K = 12.1$ mag (10 mJy) and of (*right*) ~7000 sources brighter than $K = 13$th mag (4.4 mJy). A cos $|b|$ projection has been applied. The gray regions denote areas that either have yet to be surveyed by 2MASS or have been observed but whose data was deemed to be of poor photometric quality. The total area covered is ~1000 deg^2. The diamond symbols represent cataloged galaxy clusters. The cluster of points near $l \sim 50°$ and $b \sim -0.°5$ corresponds to W51 (see Fig. 6).

(Bohlin et al. 1978; see also § 3.2), assuming that the 21 cm emission line is optically thin.

First converting the gas column density to equivalent visual extinction (multiplying by 5.3×10^{-22} cm^2; Bohlin et al. 1978; Burstein & Heiles 1982; Bernard et al. 1992) and then to an equivalent $(J-K_s)$ extinction using $E(J-K_s) = 0.54$ and $R = 3.1$, the predicted extinction nearly matches, to better than ~5%, the measured $J-K_s$ of extended sources in the ZoA for $|b| > 5°$. The lower panels in Figure 8 show the $J-K_s$ color corrected for extinction based on the H I column density, revealing a uniform color distribution down to $|b| \sim 5°$. This result is not surprising given that nearly all of the extended sources are galaxies located behind the total column of neutral hydrogen gas, and the typical $J-K_s$ color for unreddened normal galaxies is about ~1.05 (dashed line in Fig. 8; see also Jarrett et al. 2000a, 2000b). The extinction is roughly uniform above and below the Galactic plane as the northern versus southern sources have about the same color versus b distribution down to $|b| \sim 3°$.

Below 3° the extinction is undoubtedly very patchy (see, e.g., Figs. 2 and 6) and contamination from intrinsically red extended sources is severe, rendering the H I–corrected colors as unreliable—at low Galactic latitude, nebulae associated with the Milky Way dominate the integrated colors of extended sources. An alternative method at estimating the extinction within 3° of the Galactic plane is to use the mean colors of the nonextended field stars. Although there is no shortage of stars from which to estimate ensemble averages, the main disadvantage of this method is that the mean color will represent a mix of sources along the lines of sight and therefore is subject to a

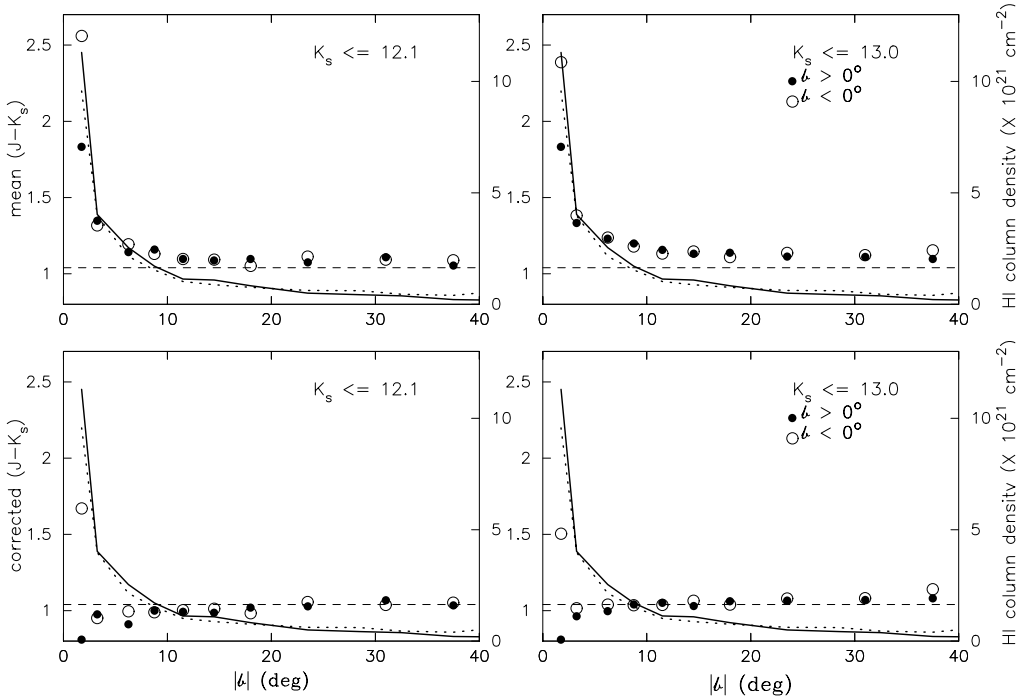

FIG. 8.—$J-K_s$ color vs. Galactic latitude. *Upper panels*: Mean $J-K_s$ color for the northern, $b > 0°$ (*filled circles*) and southern, $b < 0°$ (*open circles*) extended sources, between 40° and 70° longitude. The upper left-hand panel corresponds to sources brighter than 12.1 mag (10 mJy), and the upper right-hand panel, to sources brighter than 13th mag (4.4 mJy). For comparison, the mean hydrogen gas column density is denoted by the solid line (north) and dotted line (south). The lower panels correspond to the extinction-corrected (based on the H I column density) $J-K_s$ color. The dashed line denotes a constant color of 1.05, roughly the mean color of normal galaxies (Jarrett et al. 2000a).

wide range in dust obscuration. The solution is to use instead the colors of *extragalactic* objects, which are located behind the total column of dust of the Milky Way. Even then, this method requires a large sample of "normal" galaxies to average down systematics arising from the intrinsic color and internal extinction of the galaxy sample.

3.3.2. *Completeness and Reliability*

Producing a catalog is an exercise in balancing completeness and reliability. Flux and star-galaxy parameter thresholds are chosen to maximize the extended source completeness while also minimizing contamination from nonextended or false sources. In addition to artifacts from bright stars, the primary contaminants are double stars and triple+ stars for the Galactic plane fields. Hence, the reliability is a strong function of the stellar number density or simply background "confusion." Our strategy is to err on the side of completeness, with an *internal* completeness better than 90%, giving a larger set of extended source candidates that can then be visually examined.

Completeness, in an absolute sense, refers to the ratio of sources that are detected to the total number of sources that should be detected to some flux limit and surface brightness. In practice it is very difficult to establish the latter, since it requires an independent data set that is more sensitive and is, in itself, reliable. For "normal" early-type galaxies the 2MASS extended source catalog has been estimated to be at least 95% complete in an absolute sense for most of the sky where the stellar source density is moderate to low ($|b| > 30°$; Jarrett et al. 2000a). Note that 2MASS is *not* as sensitive to late-type spiral galaxies, including those of Sc and Sd types, particularly if they are oriented face-on, thereby decreasing their overall surface brightness (e.g., Jarrett 2000). For the Galactic plane, stellar confusion is the most significant and deleterious effect that limits both detection, characterization and discrimination, rendering a final completeness that is considerably less than 95%. The relative loss in sources (or decreasing detection rate) as a function of Galactic latitude can be estimated by measuring the "internal" completeness.

The internal completeness is defined to be the ratio or percentage of detected *and* verified extended sources that are *classified* as extended versus the total number of detected extended sources. We emphasize that for the ZoA we can only estimate the fractional loss of sources that we would normally detect at high Galactic latitude. Moreover, any "internal" measure must necessarily underestimate the true loss in sources with Galactic latitude. Some galaxies, for example, are simply not detected by 2MASS in the ZoA owing to a variety of reasons, including source confusion in which stars directly obscure the background source, bright star masking, and surface brightness. Late-type spirals are much fainter than early-type spirals or ellipticals in the near-infrared. Since we cannot reliably estimate the number of background sources that are not detected by 2MASS, any measure of "completeness" can only approximate the true completeness—more specifically, it represents an upper limit. In addition, a small percentage of sources, ~1%–3% of the total, cannot be reliably identified as stellar, Galactic, or extragalactic. Since they contribute at most only a few percent uncertainty in the completeness and reliability for $|b| > 3°$, we ignore their contribution to the overall completeness and reliability. For the most confused regions

where the fraction of "unknown" sources rises to 10%–30%, their contribution is significant (see below).

Reliability is defined to be the ratio or percentage of detected and real verified extended sources versus the sum of detected and real extended plus verified false sources that pass our "gscore" thresholding. Note that the reliability depends on the presence of real extended sources—the more extended sources there are in some region (e.g., a galaxy cluster), the higher the reliability will be—the reliability is a coupling between the density of real extended sources and the level of contamination as given by the stellar source density. For the Galactic plane, the confusion noise drives down the sensitivity, decreasing the total number of extended sources that are detected, while at the same time the number of sources that dominate contamination is on the rise. Hence, the reliability is a strong function of the stellar number density. As with the completeness calculation, sources classified as "unknown" are ignored here, representing a statistically insignificant number of sources for $|b| > 3°$.

Figure 9 shows the achieved internal "completeness" and reliability for the combined "north" and "south" catalogs. We have not applied any corrections for extinction. The internal completeness holds steady between 90% and 95% for most of the ZoA. The reliability also holds steady between 90% and 95% all the way down to $|b| \sim 5°$–$7°$ (corresponding to 10^4 stars deg^{-2} brighter than 14th mag at K_s). But, as the confusion noise dramatically rises for $|b| < 5°$, the reliability decreases to $\sim$40%. Note also that the 40% reliability is *inflated* owing to the presence of W51, a large source of fuzzy objects less than 1° from the Galactic plane.

Since the actual total number of sources is small, it is feasible to inspect each extended source candidate visually and eliminate most of the false sources (e.g., multiple stars) yielding a *corrected* reliability greater than 90%. There will still remain a large number of sources whose nature cannot be discerned from visual inspection or otherwise using 2MASS parametric information: $\sim$28% of the extended sources at $|b| < 3°$ are classified as "unknown." These sources can significantly alter the true reliability. But as a final note, we should point out that the very definition of what is "extended," at least with respect to the PSF, breaks down as the source density blows up near the Galactic plane. In the Galactic center, just about everything is "extended" as nebulosity and walls of stars merge in projection on the sky.

3.3.3. *Source Counts*

Figure 10 shows the cumulative number of extended sources per deg^2 for flux thresholds $K_s = 12.1$ and 13.0 (4 and 10 mJy, respectively). We have not applied any corrections for dust extinction. The northern sample ($b > 0°$) is denoted with filled circles, and the southern sample ($b < 0°$), with open circles. Three trends are clear: (1) an "excess" of

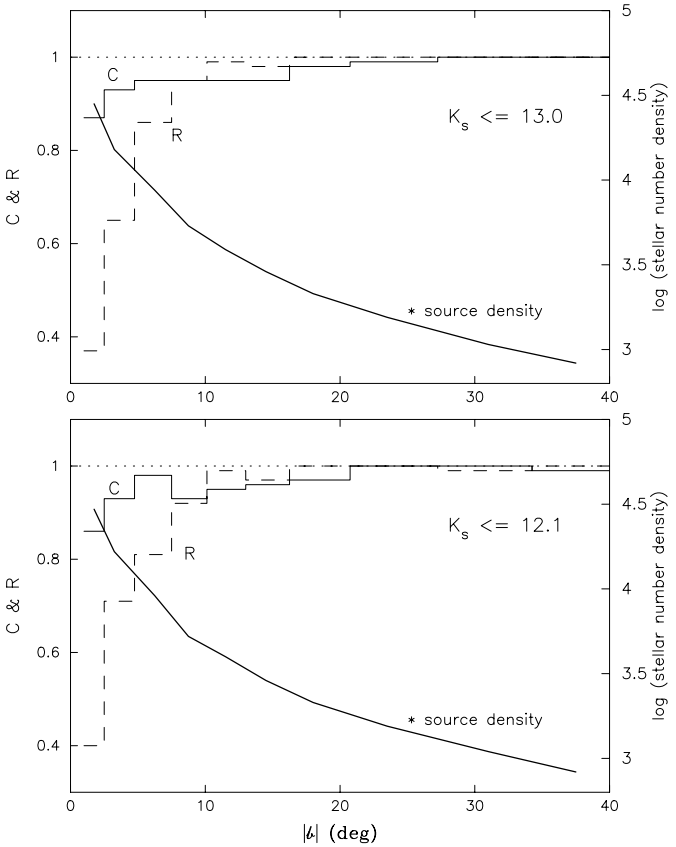

FIG. 9.—Completeness and reliability of the combined, $|b| < 40°$ and l between 40° and 70°, extended source catalog. The internal completeness (see text for definition) is denoted with a solid line, and the reliability with a dashed line. The upper panel corresponds to sources brighter than 13th mag (4.4 mJy), and the bottom panel, to sources brighter than 12.1 mag (10 mJy). For comparison, the stellar number density (stars per square degree brighter than 14th mag at K_s) is denoted with a thick solid line.

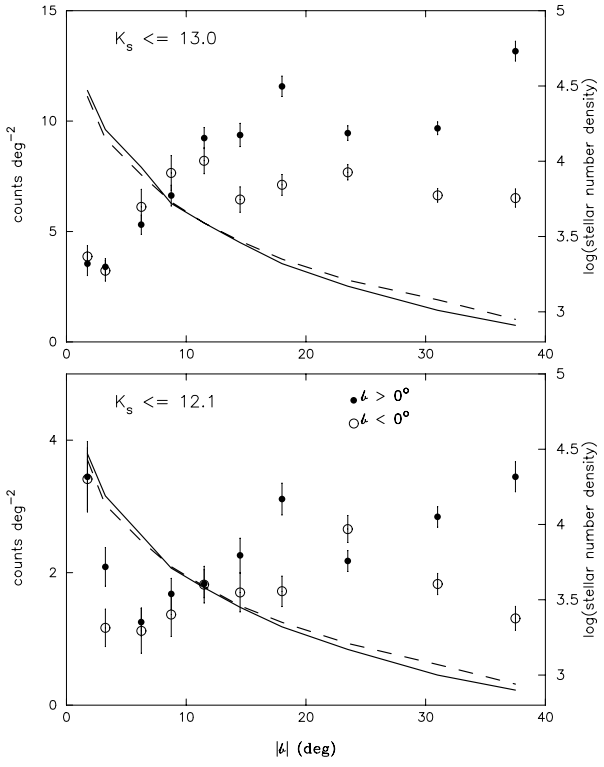

FIG. 10.—Extended source area-normalized cumulative counts for the northern, $b > 0°$ (*filled circles*) and southern, $b < 0°$ (*open circles*), fields between 40° and 70° longitude, extended sources. The upper panel corresponds to sources brighter than 13th mag (4.4 mJy), and the bottom panel, to sources brighter than 12.1 mag (10 mJy). The error bars represent the $\sqrt{n}$ statistical uncertainty. For comparison, the stellar number density (stars per square degree brighter than 14th mag at K_s) is denoted with a thick solid line (north) and dashed line (south).

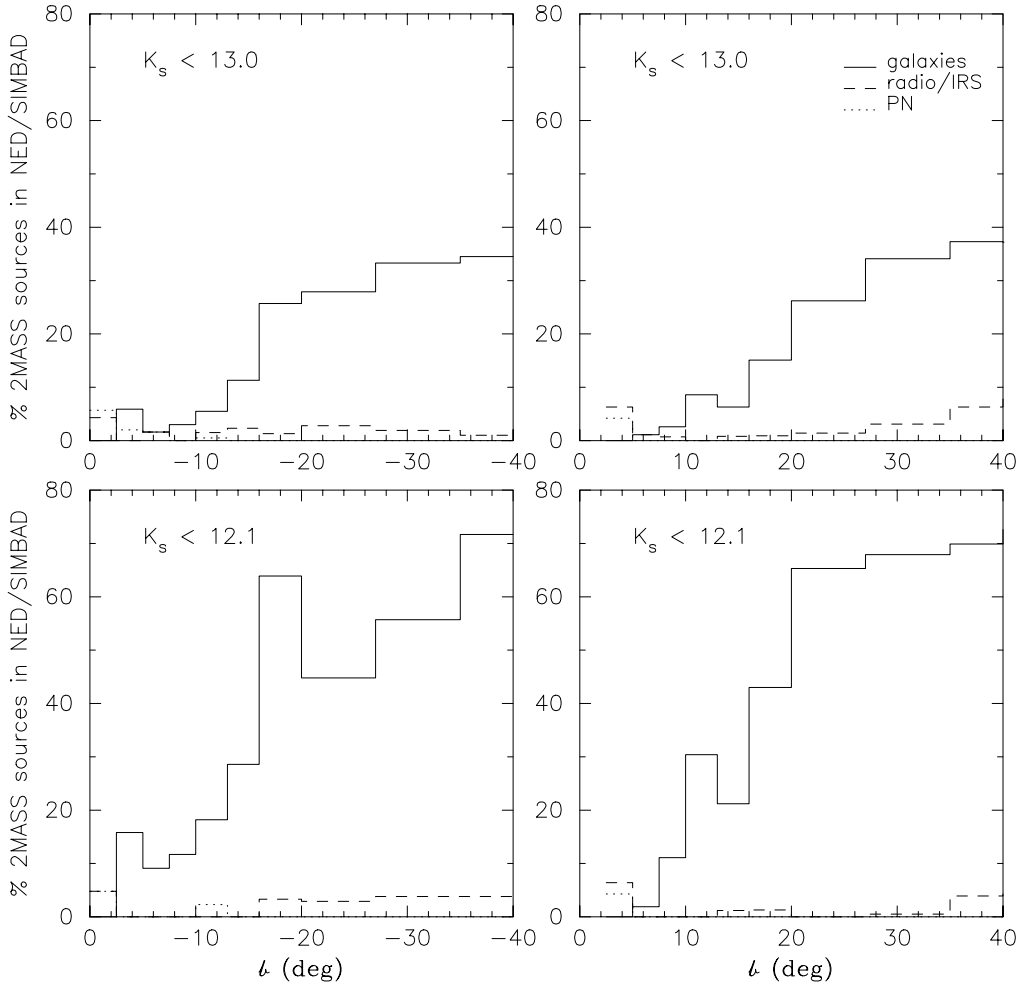

FIG. 11.—Percentage of 2MASS extended sources found in the NED and SIMBAD databases, separated according to whether the source is a confirmed galaxy, Galactic planetary nebula, or a radio/infrared source (which are also typically Galactic in origin). The upper left-hand panel corresponds to sources brighter than 13th mag (4.4 mJy), and the bottom panel, to sources brighter than 12.1 mag (10 mJy), for the southern extended sources ($b < 0°$). The upper right-hand panel corresponds to sources brighter than 13th mag (4.4 mJy), and the bottom panel, to sources brighter than 12.1 mag (10 mJy), for the northern extended sources ($b > 0°$). Both data sets are confined to the Galactic longitude range between 40° and 70°.

sources between +30° and +40° latitude, (2) declining counts between 5° and 12° latitude, and (3) an upturn in the declining source counts for bright sources near the Galactic plane, $|b| < 3°$. The average trend for $|b| > 5°$ is about eight to 10 galaxies per deg^2 brighter than 13th mag at K_s and about one to two galaxies per deg^2 brighter than 12th mag at K_s. Finally, there is statistically significant difference between the source counts in the northern ($b > 0°$) and southern ($b < 0°$) fields. The asymmetry is most likely due to real large-scale structure from background galaxy clusters.

The excess at high Galactic latitude comes from the presence of a number of prominent galaxy clusters (see Fig. 7). A large-scale structure, extending from 2000 to 5000 km s^{-1}, has been previously identified by Marzke, Huchra, & Geller (1996). More generally, the northern galaxy counts ($b > 0°$) tend to be greater than those of the south ($b < 0°$), highlighting the apparent "wall" of galaxies to the north of the Galactic plane.

The 30%–50% decline in source counts between 5° and 12°, corresponding to an increase in stellar number density of 3200 to 10,000 stars per deg^2 brighter than 14th mag at K_s, tracks the increasing background confusion noise and subsequent loss in completeness for *extragalactic* objects. The extended source completeness, specifically the internal component, was first shown in Figure 9 to be ~85%–90% for $|b| < 10°$. Since the number counts measure both the internal and absolute completeness, assuming a smooth spatial distribution of galaxies, we infer that 2MASS is not detecting from 15% to 35% of the total possible number of extended sources (i.e., galaxies) brighter than 12th mag at K_s deep in the ZoA, $|b| \sim 5°$ and $l \sim 50°$.

The upturn in the source counts for bright sources at low Galactic latitude, $|b| < 3°$, is due to foreground Galactic nebulae, including H II regions, planetary and diffuse nebulae, which are predominantly confined to the Galactic plane near $|b| = 0°$. The W51 GMC is the most prominent cluster of Galactic nebulae and dense clusters of young stars in the study area (cf. Fig. 6). At these source densities, more than 20,000 stars per deg^2 brighter than 14th mag at K_s, the confusion noise is so large that detection of background galaxies is limited to only the nearest or intrinsically brightest galaxies (e.g., Fig. 5). Conversely, star formation regions, and most GMCs, tend to be confined to the Galactic plane with scale heights less than 0.1 kpc. Both effects result in an excess of extended source counts deep in the ZoA, at least for $l \sim 50°$, with patchy variation throughout the disk of the Milky Way.

3.3.4. *Previously Cataloged Extended Sources*

The NASA Extragalactic Database (NED) provides a means for comparison between 2MASS galaxy detections and previously cataloged extragalactic sources. The primary objective is to estimate the number of new galaxies that 2MASS will add to NED and, in particular, to the traditionally incomplete ZoA. We also utilize SIMBAD to search for Galactic extended objects (e.g., H II regions), which are a significant component to the total number of extended sources at the highest source densities. Figure 11 summarizes the 2MASS versus NED/SIMBAD cross-comparison. Here we have split the extended sources into (1) galaxies, (2) radio and infrared sources (which may also be galaxies, but are more likely Galactic in nature), and (3) planetary nebulae. The left-hand upper/lower panels correspond to the southern fields ($b < 0°$), and the right-hand upper/lower panels, to the northern fields ($b > 0°$). For $b > 20°$, upward of 30%–60% of the 2MASS sources are previously cataloged galaxies—most of which belong to the cluster of galaxies discussed in § 3.3.3. The percentage drops dramatically as we enter the ZoA, where only 5%–25% are previously cataloged galaxies for $5° < |b| < 20°$. For *galaxies*, the percentage drops to zero near the Galactic plane. The number of radio/infrared and planetary nebulae increases to 5%–10% of the total at these extreme stellar source densities. It is likely that the true percentage of Galactic extended sources at $|b| < 3$ is at least 50%, reflecting the incompleteness of previously catalogued sources in the Galactic plane.

4. DISCUSSION

The plane of the Milky Way presents a number of obstacles toward detection of background galaxies. At optical wavelengths, the dust obscuration attenuates the already diffuse light coming from galaxies (relative to stars). At longer wavelengths, such as the far-infrared (e.g., *IRAS*), the dust is transparent, but limitations arising from spatial resolution and sensitivity result in missed sources. Radio surveys provide a clear window toward detection of nearby gas-rich (i.e., late-type spiral) galaxies but currently lack the sensitivity to detect more distant spirals ($cz > 5000$ km s^{-1}) or gas-poor early-type galaxies. The near-infrared, in contrast, offers a sort of compromise between the optical and radio bands. Dust attenuation is an order of magnitude less at 2.2 μm compared to optical bands, while the spatial and sensitivity limits of surveys such as 2MASS and DENIS allow detection of both spiral and elliptical galaxies background to the ZoA out to redshifts $\sim$10–20,000 km s^{-1} (cf. Kraan-Korteweg et al. 1998; Mamon et al. 1999; Schroeder, Kraan-Korteweg, & Mamon 1999). As demonstrated in Figure 11, 2MASS will increase the number of new galaxy detections in the ZoA by a factor of $\geq$3. Moreover, for galaxies brighter than 12.1 mag (10 mJy) and sizes greater than 14″, 2MASS will provide a complete ($\sim$80%–90%) sample at a rate of about two galaxies per deg^2 penetrating the ZoA down to $|b| \sim 5°$. Lifting the veil of the Milky Way, a more complete map of large-scale structure will be possible with follow-up redshift observations of 2MASS galaxies.

Given the detection rate in this region of the Milky Way, we estimate the total number of galaxies that 2MASS will find in the entire ZoA, excluding $\pm 20°$ around the Galactic center. Integrating the rates for $|b| < 20°$ gives between 12,600 and 25,000 galaxies brighter than 12.1 mag (10 mJy) at K_s, and deeper in the plane, $|b| < 10°$, between 6400 and 12,800 galaxies brighter than 12.1 mag (10 mJy) at K_s. From 75% to 95% of these galaxies will be newly cataloged by 2MASS, with a reasonable fraction having H I counterparts coming from the deep 21 cm surveys. We may expect more new galaxies since the region studied in this work, $40° < l < 70°$, has a much higher stellar density, translating to higher confusion noise and lower sensitivity, than in the Galactic anticenter region. Moreover, the ZoA region studied here is likely to be *underdense* in galaxies in comparison to the anticenter/supercluster fields and the region encompassing the Great Attractor (e.g., Kolatt, Dekel, & Lahav 1995). We expect many of these sources to be in common with ongoing H I surveys, although it is worth noting that none of the Arecibo H I detections in the present work is sufficiently strong that they would have been detected in the shallow H I surveys of the past few years. We can expect at least half to be detected only by 2MASS.

The 2MASS census of galaxies in the ZoA will provide the necessary information toward identification of galaxy clusters veiled by the Milky Way. These clusters in turn will help establish the large-scale structures extending into the ZoA and probe the mass density of the Hydra-Centaurus-Pavo-Indus-Telescopium wall of galaxies. By relating the observed infall velocity to the distribution of matter, we can estimate the mean mass density of the universe.

The redshift distribution for previously cataloged galaxies and from this work is given in Table 1 and illustrated in Figure 12, ranging between 2000 and 50,000 km s^{-1}. It should be noted that many of the galaxies in Table 1 have redshifts between 5000 and 8000 km s^{-1}, which is where we would expect an *extension* of the large-scale "Great Wall" (Geller & Huchra 1989) to be located *if* the western extent (see Marzke et al. 1996) were beginning to close off as another "bubble" feature. Although the distribution is not from a complete sample of galaxies, the results do show peaks for galaxies at 5500 and at 8500 km s^{-1}. In spatial projection (Fig. 7) we see large angular scale structures extending from $b \sim 35°$ down to 20° (but may extend as far as 10°), with a clear clustering of galaxies near $l \sim 60°$ and $b \sim 19°$. Unfortunately the current gaps in the 2MASS

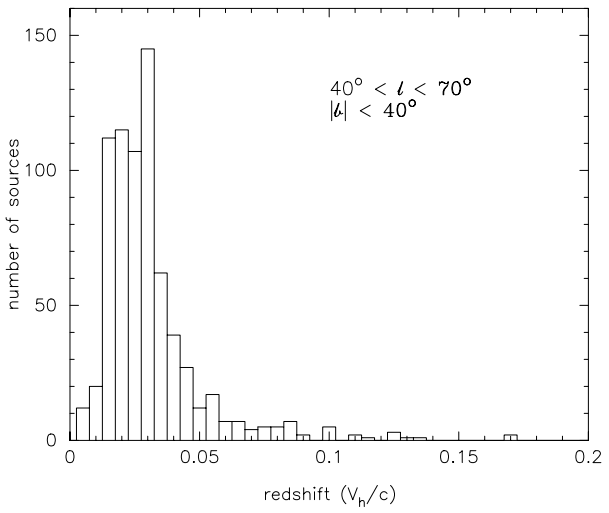

FIG. 12.—Redshift distribution for previously cataloged galaxies (via NED) and from this work (Table 1). Note the peaks at 5500 and 8500 km s^{-1}.

coverage hides the true extent of this cluster, as well as any large-scale structures in the southern fields. The more complete 2MASS map, which will be available in the near future, and a more complete redshift census of galaxies in these fields, is required to substantiate this hypothesis. Finally, redshift-independent distance measures (e.g., *H*-band Tully-Fisher) are needed to establish cluster space densities that are nonbiased.

Not only will 2MASS and DENIS help reveal large-scale structures hidden behind the Milky Way, it is still possible that a large previously undetected Local Group galaxy will be uncovered by these near-infrared survey or the H I surveys in upcoming years as these surveys reach their peak in productivity. A galaxy comparable in size to that of M31 will have enough mass to play a significant role in the gravity field of the Local Group, conceivably the source of complex and puzzling peculiar velocities observed in the Local Group and other nearby groups. It is more likely that smaller Local Group galaxies will be discovered, a prospect that would also be important to understanding these galaxies. Already 2MASS has discovered large angular-sized galaxies *near* the Local Group (Hurt et al. 2000; Howard 2000). What we can say with confidence is that the zone of avoidance is now a zone of discovery.

5. SUMMARY

Some ~ 1000 deg^2 surveyed by 2MASS between 40° and 70° Galactic longitude and $\pm 40°$ about the Galactic plane include over 7000 verified extended sources brighter than 13.0 at K_s (4.4 mJy) and more than 1600 sources brighter than 12.1 at K_s (10 mJy). For the ZoA, $|b| < 20°$, most of the sources are newly discovered, with a small fraction, $\sim 5\%$–25%, previously cataloged in NED. For a number of new 2MASS galaxies we acquired confirmation observations, including deep *K*-band imaging and spectroscopy at *I*-band and radio wavelengths.

On average, 2MASS discovers galaxies at the rate of about eight to 10 per deg^2 brighter than 13th mag (4 mJy) at K_s and about two galaxies per deg^2 brighter than 12th mag (10 mJy) at K_s. Near the Galactic plane, $|b| < 3°$, the extended source counts are dominated by Galactic H II regions and large low surface brightness nebulae. The W51 GMC ($l \sim 49°$, $b \sim -0.°5$) is clearly detected and split into dozens of 2MASS extended sources. Most important, 2MASS discovers new galaxies near the Galactic plane, at least down to stellar source densities as high as 10,000 stars per deg^2 brighter than 14th mag at K_s. At the final completion of the 2MASS survey, we project that over 20,000 "normal" galaxies will be detected in the ZoA, $|b| < 20°$, at least half of which will be detectable in H I in deep 21 cm radio surveys.

We thank Glenn Veeder for help in obtaining the Palomar near-infrared observations and Perry Berlind and Mike Calkins for optical spectroscopy. We thank Raymond Tam with help in galaxy classification. Ron Beck, Diane Engler, and Helene Huynh were instrumental in gathering 2MASS image data. We thank Geraldine Jarrett for text editing. Finally, we thank Daniel Egret for providing fast access to the SIMBAD database. The Digitized Sky Surveys were produced at the Space Telescope Science Institute. This research has made use of the NASA/IPAC Extragalactic Database (NED) which is operated by the Jet Propulsion Laboratory, California Institute of Technology, under contract with the National Aeronautics and Space Administration (NASA). This publication makes use of data products of the 2MASS, which is a joint project of the University of Massachusetts and the Infrared Processing and Analysis Center, funded by the NASA and NSF. This work was supported in part by the Jet Propulsion Laboratory, California Institute of Technology, under a contract with NASA.

REFERENCES

Aaronson, M., Huchra, J., Mould, J., Schechter, P. L., & Tully, R. B. 1982, ApJ, 258, 64
Bernard, J., Boulanger, F., Desert, F., & Puget, J. 1992, A&A, 263, 258
Bohlin, R., Savage, B., & Drake, J. 1978, ApJ, 224, 132
Branchini, E., et al. 1999, MNRAS, 308, 1
Burstein, D., & Heiles, C. 1982, AJ, 87, 1165
Carpenter, J., & Sanders, D. 1998, ApJS, 116, 1856
Canavezes, A., et al. 1998, MNRAS, 297, 777
da Costa, L. N., et al. 1994, ApJ, 424, L1
de Lapparent, V., Geller, M. J., & Huchra, J. P. 1986, ApJ, 302, L1
de Vaucouleurs, G., de Vaucouleurs, A., Corwin, H. G., Buta, R., Paturel, G., & Fouque, P. 1991, Third Reference Catalogue of Bright Galaxies (New York: Springer)
Di Nella, H., Couch, W., Parker, Q., & Paturel, G. 1997, MNRAS, 287, 472
Epchtein, N., et al. 1997, Messenger, 87, 27
Faber, S. M., & Burstein, D. 1988, in The Vatican Study Week on Large Scale Motions in the Universe, ed. G. V. Coyne & V. C. Rubin (Princeton: Princeton Univ. Press), 115
Fisher, K. B., Huchra, J. P., Strauss, M. A., Davis, M., Yahil, A., & Schlegel, D. 1995, ApJS, 100, 69
Geller, M., & Huchra, J. 1989, Science, 246, 897
Giovanelli, R., & Haynes, M. 1988, in IAU Symp. 130, Large Scale Structures in the Universe, ed. J. Audouze, M. C. Pelletan, & A. Szalay (Dordrecht: Reidel), 113
Hartmann, D., & Burton, W. B. 1997, Leiden/Dwingeloo Survey of H I in the Galaxy (Cambridge: Cambridge Univ. Press)
Henning, P. 1992, ApJ, 78, 365
Henning, P., et al. 1998, AJ, 115, 584
Henning, P., Staveley-Smith, L., Kraan-Korteweg, R., & Sadler, E. 1999, Publ. Astron. Soc. Australia, 16, 1
Howard, E. 2000, AJ, submitted
Hurt, R., Jarrett, T. H., Kirkpatrick, D., Cutri, R. M., Skrutskie, M., Schneider, S., Skrutskie, M., & van Driel, W. 2000, AJ, in press
Jarrett, T. H., Chester, T., Cutri, R., Schneider, S., Skrutskie, M., & Huchra, J. 2000a, AJ, 119, 2498
———. 2000b, in preparation
Jarrett, T. H. 2000, PASP, in press
Juraszek, S. 1999, Publ. Astron. Soc. Australia, 16, 1
Kaiser, N., et al. 1991, MNRAS, 252, 1
Kilborn, V., Webster, R. L., & Staveley-Smith, L. 1999, Publ. Astron. Soc. Australia, 16, 8
Kolatt, T., Dekel, A., & Lahav, O. 1995, MNRAS, 275, 797
Koo, B. C. 1997, ApJS, 108, 489
———. 1999, ApJ, 518, 760
Kraan-Korteweg, R., et al. 1994, Nature, 372, 77
———. 1996, Nature, 379, 519
Kraan-Korteweg, R., & Huchtmeier, W. 1992, A&A, 266, 150
Kraan-Korteweg, R., Schroeder, A., Mamon, G., & Ruphy, S. 1998, in The Impact of Near-IR Surveys on Galactic and Extragalactic Astronomy, ed. N. Epchtein (Dordrecht: Kluwer), 209
Kraan-Korteweg, R., & Woudt, P. 1999, Publ. Astron. Soc. Australia, 16, 1
Lahav, O., Yamada, T., Scharf, C., & Kraan-Korteweg, R. 1993, MNRAS, 262, 711
Lu, N., Dow, M., Houck, J., & Salpeter, E. 1990, ApJ, 357, 388
Lu, N., & Freudling, W. 1995, ApJ, 449, 527
Lynden-Bell, D., et al. 1988, ApJ, 326, 19
Mamon, G., Borsenberger, J., Tricottet, M., & Banchet, V. 1998, in The Impact of Near-IR Surveys on Galactic and Extragalactic Astronomy, ed. N. Epchtein (Dordrecht: Kluwer), 177
Marzke, R., Huchra, J., & Geller, M. 1996, AJ, 112, 1803
Nakanishi, K., et al. 1997, ApJ, 112, 245
Oliver, S., et al. 1996, MNRAS, 280, 673
Pantoja, C., Altschuler, D., Giovanardi, C., & Giovanelli, R. 1997, AJ, 113, 905
Rowan-Robinson, M., et al. 1990, MNRAS, 247, 1
Saunders, W., et al. 1991, Nature, 349, 32

Schneider, S. E., Thuan, T., Mangum, J., & Miller, J. 1992, ApJS, 81, 5
Schroeder, A., Kraan-Korteweg, R., & Mamon, G. 1999, Publ. Astron. Soc. Australia, 16, 1
Skrutskie, M., et al. 1997, in The Impact of Large Scale Near-IR Sky Surveys, ed. F. Garzon et al. (Dordrecht: Kluwer), 25
Smoot, G., Gorenstein, M., & Muller, R. 1977, Phys. Rev. Lett., 39, 898
Staveley-Smith, L. 1997, Publ. Astron. Soc. Australia, 14, 111
Staveley-Smith, L., et al. 1998, AJ, 116, 2727